Letters in High Energy Physics

ISSN: 2632-2714

Microstructure and Hardness of Aluminum Silicon Iron and Aluminum Chromium Iron Functionally Graded Alloys

Haydar Al-Ethari 1*, Abdul Raheem Kadhim Abid Ali 2, Ali Abbas Hasan 3

Abstract

Functionally graded materials provide much better performance than materials with fixed properties and compositions. In this study aluminum-based alloys were used to prepare FGM. Al-Si-Fe eutectic composition and Al-Cr-Fe alloys were proposed for this work, Possible applications of these materials are suggested, as automotive pistons or cylinders block. FGM was fabricated by successive stages of stir casting method during the solidification, the mold was subjected to mechanical vibration many. Mechanical and physical tests were carried out such as XRD, microstructure, hardness tests to evaluate the performance of this material. FGM samples were prepared by sequential casting of the tow alloys (Al-Si-Fe) and (Al-Cr-Fe). Two types of samples were studied and compared, with and without mold vibration.

Keywords: aluminum alloys, gravity casting, sequential casting, interface, mechanical vibration

1. Introduction

Functionally graded materials (FGMs) sophisticated composite materials used engineering that display a spatial variation in composition and/or shape in order to meet specified criteria. Three distinct categories of FGMs exist [1]: chemical composition gradient FGMs, microstructural gradient FGMs, and porosity gradient FGMs. The chemical composition gradient of FGMs involves a progressive variation of the chemical composition along the spatial location inside the material. The microstructure gradient fiber-reinforced composites FGMs exhibit a distinct microstructural variation within a single material. This variation is intentionally designed to achieve certain qualities in specific regions of the material. These materials have been utilized in several technical domains, including aerospace, nuclear, electrical, biomedical, defense, and automotive industries [2].

Metal alloys are commonly employed in the automobile sector. The rise of the aluminum alloys business been primarily driven by the aircraft and automobile industries, as a result of stricter environmental laws [3-20]. Cast aluminum alloy automobile components, such pistons, engine blocks, and rocker coves, are commonly observed in everyday cars [4-18]. The structural component

production business is mostly influenced by permanent mold casting processes. Aluminum alloys are considered to be a category of sustainable materials due to their recyclability, cost-effectiveness, lightweight nature, weldability, and superior mechanical strength [5].

Recent studies have proposed the use of gravity casting as a method for manufacturing aluminium -FGM pistons [6-7]. These pistons are designed with a dual composition, consisting of Al-Si-Fe in the piston crown to enhance mechanical strength and thermal resistance, and Al-Cr-Fe in the piston skirt to enhance ductility. Pistons, frequently fabricated using the silicon alloy Al-Si-Fe are frequently experience fatigue cracking in the skirt because of the alloy's limited ductility [8]. Moreover, the inclusion of silicon (Si) in these alloys, whether it is present in intermetallic phases or not, can have an impact on the wear resistance. The study conducted by provided evidence of the impact of Si particles on the wear rate of aluminum-silicon alloys[8-9].

The automotive industry requires high quality castings and the ability to produce on a large scale. This requires evidence that the connection between the alloys in the FGM process is not subject to any defects or failures that may lead to failure of the design [10]. In this study we examined the

¹ Department of Metallurgical Eng., Materials Eng. College, University of Babylon, Babylon, Iraq

² Department of Metallurgical Eng., Materials Eng. College, University of Babylon, Babylon, Iraq

³ Department of Metallurgical Eng., Materials Eng. College, University of Babylon, Babylon, Iraq

^{*} Corresponding author's e-mail: dr.eng.alethari@uobabylon.edu.iq

Letters in High Energy Physics

ISSN: 2632-2714

properties of aluminum and aluminum FGMs produced using gravity casting. In order to evaluate the quality of bonding, create intermetallic compounds, and evaluate the effectiveness of these alloys in performing their assigned function, the metallic bonding between the two alloys was examined through the use of micro hardness tests, and SEM impact testing, microstructure analysis[11]. This study used a combination of mechanical characterization and intermineral monitoring techniques to effectively identify and confirm potentially important issues. Some researchers have studied the vibration method with casting. Energy is introduced into the casting through a device that generates mechanical energy due to vibration. This method brings many benefits, such grain refinement and reducing defects and isolations within the alloy, and it is also supposed to help in the distribution of elements when manufacturing FGM[12-16].

It is possible to study the preparation of functionally graded materials with s through

sequential stir casting method with a solidification under the effect of mechanical of vibration. The FGM is to be prepared using aluminum-silicon based alloys the sources of which is an engine parts and aluminum-chromium alloys prepared in this study[13-21].

2. Materials and Methods

Two different aluminum alloys were used to realize the castings, the first coded as C1 is Al-Si-Fe alloy, having the chemical composition shown in table (1),this alloy was prepared used some failed parts of the IC engine with chemical composition after melting shown in Table (2). The alloy is coded as C2. The C1 alloy was pried by adding 2wt% of Fe to the C2 alloy by stir casting method. The second alloy, coded as C3 was prepared as Al-Cr-Fe by stir casting method by adding 8 wt% chromium and 2 wt% Fe to pure aluminum, Table (3) shows the chemical composition of this alloy.

Element Si Cr Fe Cu Mn Mg Al% Coad C 1 12 0 2 0.02 0.8 0.05 Bal. C 2 12.4 0 0.9 0.07 0.03 Bal. C 3 0 8 2 0.01 0.026 0.2 Bal.

Table 1. chemical composition of alloys.

The melting process was carried out at 950° C in a gas furnace, emitting inert argon gas to isolate the melt from surrounding contamination. Mixing operations took place during the melting process. The alloy elements were coated with foil and gradually added to the melt. Mechanical mixing was used at a speed of 30 rpm to ensure the distribution of the elements within the alloy until the pouring process.

A steel mold heated to 450° C with a cylindrical cavity of 24 mm diameter and 150 mm height was used in serial casting to produce the FGM specimen.

The first alloy, Al-Cr-Fe, was cast, while the second alloy, Al-Si-Fe, was cast sequentially. A key factor is the time elapsed between casting the first and second alloy, which is 20 seconds [14]. The casting temperature was set at 900 °C for both

alloys. The first alloy must present a temperature already below the fluid line to avoid mixing of the two alloys, but at the same time it must be above the solidus line. If the temperature is too low, the danger is that a break will occur between the two alloys after solidification.

The mold was mechanically shaken while the mold hardened. Mechanical vibrations were provided using the vibration device shown in Figure 1.[15-17]. The device provides vibrations due to the shaft with an eccentricity equal to 1.50 mm. The shaft was rotated at a rotational speed of 600 rpm to obtain the desired frequency. Due to eccentricity, the table in which the mold is attached to the device vibrates vertically with a designed amplitude equal to the eccentricity and the vibration process continues until the melt solidifies inside the mold.

ISSN: 2632-2714

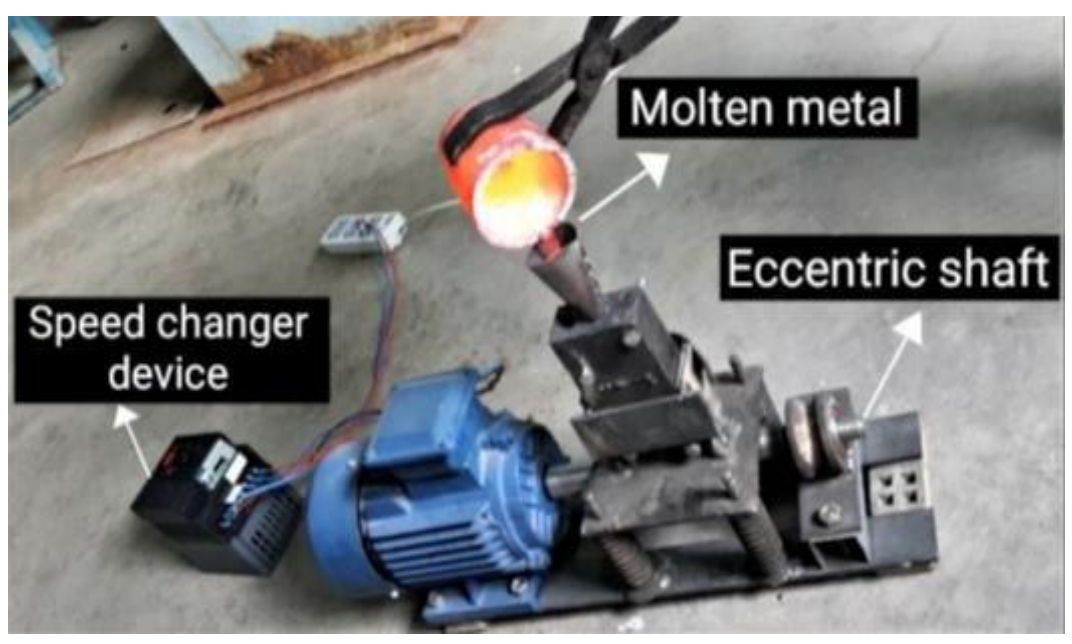


Figure 1. vibration divas system[7]

3. Physical and mechanical tests

3.1. Microstructure analyses

The test carried out for the prepared FGM sample Specimens with a length of (130 mm) was used. The specimen was flattened using SiC grinding papers having different roughness (400, 800, 1000, 1200, 2000, grit size). Grinding and polishing operations were done using polishing machine model (MP-2B grinder polisher). The Al-Cr-Fe alloy specimens were etched by (5ml HF, 195ml Distilled water) for (15 second) while, Al-Si-Fe alloy specimens were etched by (2ml HF, 3ml HNO3, 5ml HCl Distilled 190ml water) for (15 second) at room temperature[11], then the specimens were washed with distilled water, and dried by electric dryer. An optical microscope was used with suitable magnification of 400X to examine the microstructure of each specimen. test were conducted at room temperature with rate of Compression (0.5 mm/min) .

3.2. SEM-EDS Test:

Surface analyses, chemical analysis and imaging for sample wear performed using SEM/EDS test. Surface for tested specimen were prepared in similar manner to that of optical microscopy at interface zone. The Scanning Electron Microscope is equipped with an Energy Dispersive Spectrometer (EDS). EDS provides chemical analysis of the field of view or spot analyses of

minute particles. The analysis had been carried via device Type (inspect F50)

3.3. X-ray Diffraction (XRD)

Specimens with (20 x 10mm) at interface zone were prepared for X-ray diffraction analysis. The measure conditions are Target: Cu, wave length of 1.54060 , voltage and current are 30 KV and 15 mA respectively, Scanning step of 0.05 with a step time of 2 s, and a scanning range of (5°-80°) were used.

3.4. Vickers Hardness Test

The Vickers hardness test was carried out according to ASTM (E10-15a), with a load of 10 Kg. Appropriate grinding and polishing were carried out before subjecting the specimens to the test. The test was performed at every 5 mm along the specimens length of 130 mm, At the interface region the test were carried out at every 0.25 mm. The test was carried out via a hardness tester type (HVS-1000). Test were conducted at room temperature with rate of Compression (0.5 mm/min).

4. Results and Discussion

4.1. Microstructure

The optical microscope image of FGM alloys C1-C3 showed the microscopic structure at the interface area where the two alloys met. When aluminum melts in the presence of alloying

elements, the phases will precipitate. The intermetallic compound cannot form a solid solution with the aluminum, so it remains implanted in an alloy suchas $\beta\text{-Al5FeSi}$, Al95Fe4C , Al80Cr20 . The silicon is clear and flakes appear in the $\alpha\text{-Al}$ matrix. The difference in structure is clear through the morphology, phases, and the presence of intermetallic compounds, the presence of which was confirmed by the XRD results. Microstructure examination was carried out on

samples under the influence of vibration in Figure (2) and without vibration in Figure (3), the tow samples as cast without any heat tremens It is clear that there is a difference in the microscopic structure, as the sample with vibration has less gran size and there is no pores, and there is a clear effect on the intermetallic compound, as its morphology changed and the flakes became smaller in size. It is not continuous and is more widely distributed in the alloy.

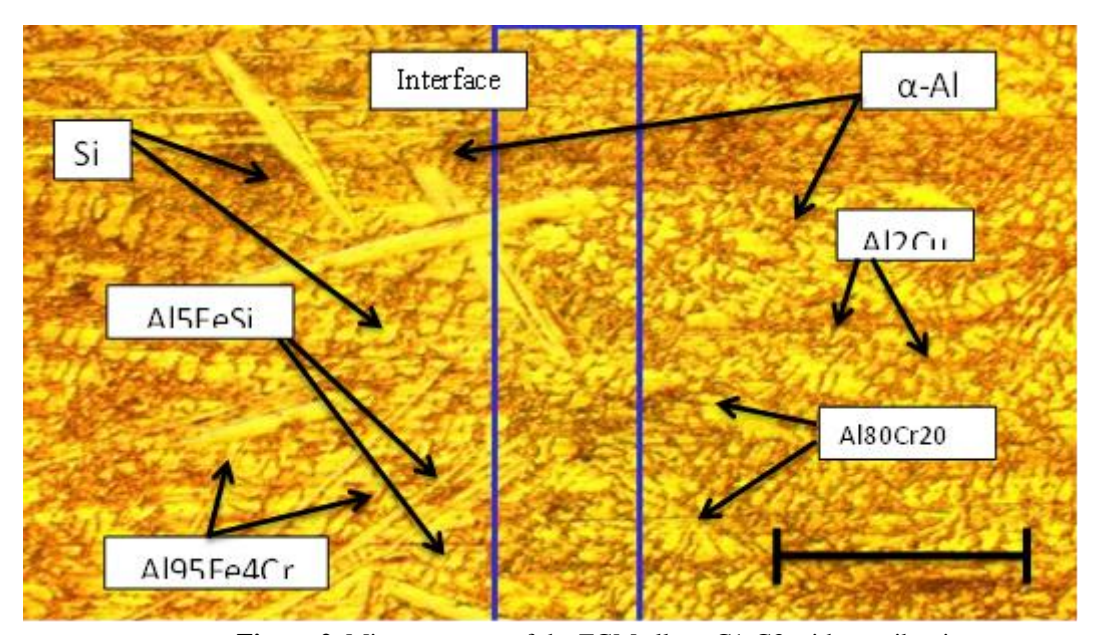


Figure 2. Microstructure of the FGM alloys C1-C3 without vibration

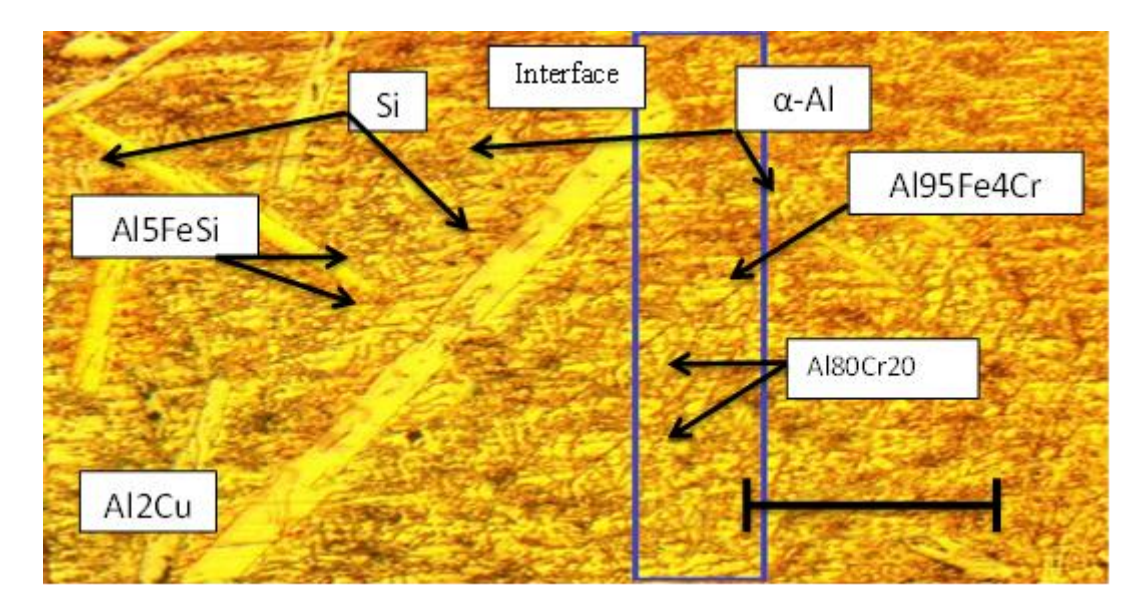


Figure 3. Microstructure of the FGM alloys C1-C3 with vibration

4.2 X-Ray Diffraction Analysis

The charts of the X-ray diffraction pattern for sample at the interface zone of the prepared functionally graded alloy is shown Figure (4). The

peaks match with the standard chart XE82 of the X-ray diffraction for each phase

The result shown included $\,$ α -Al phase, Si, β -Al5FeSi, Al80Cr20, Al95Fe4Cr and Al2Cu.

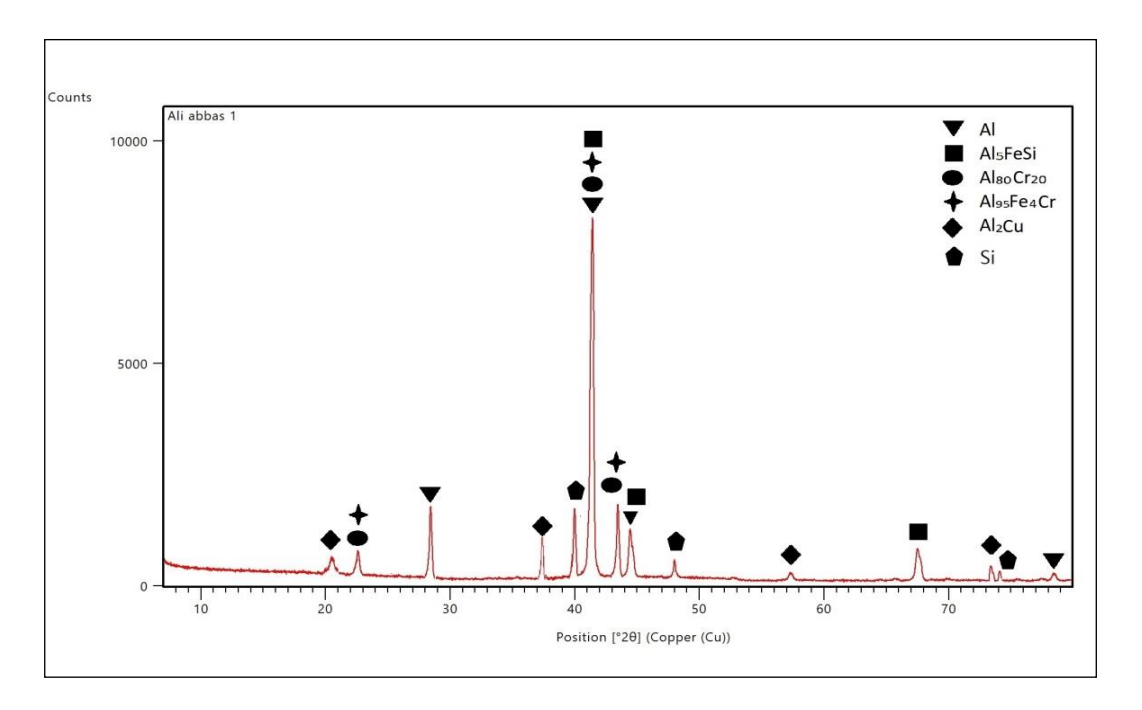


Figure 4. XRD Analysis FGM sample (C1-C3)

4.3. SEM-EDS Analysis

Figure (5) a shows the interface between FM (C1-C3) alloy without the vibration effect, and Figure (6) with the vibration effect. It can be observed that there is no defect to be seen or loss of contact, the α -Al phase as the base contains the Other.

Al80Cr20, appears in the form of circular or equiaxed precipitates[15]. Al95Fe4Cr, in the form of a longitudinal crystal[15]. β -Al5FeSi in the form of chips distributed on the C1 alloy, Al2Cu, where the particle size is less than the large β -Al5FeSi, Sharpe precipitates[15].

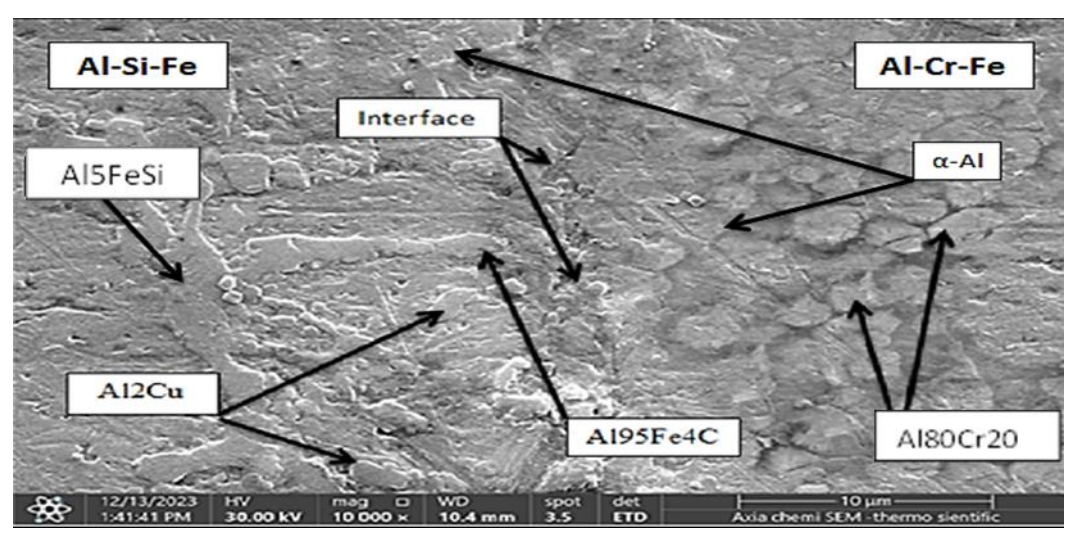


Figure 5. SEM image at interface of of FG sample (C1-C3) with vibration

It can be detected that the sample with vibration effect have an improvement in the microstructure and morphology of the intermetallic component and silicon, it changed to a smaller, non-

continuous form and is more widely distributed in the alloy, which is effected on the properties and performance.

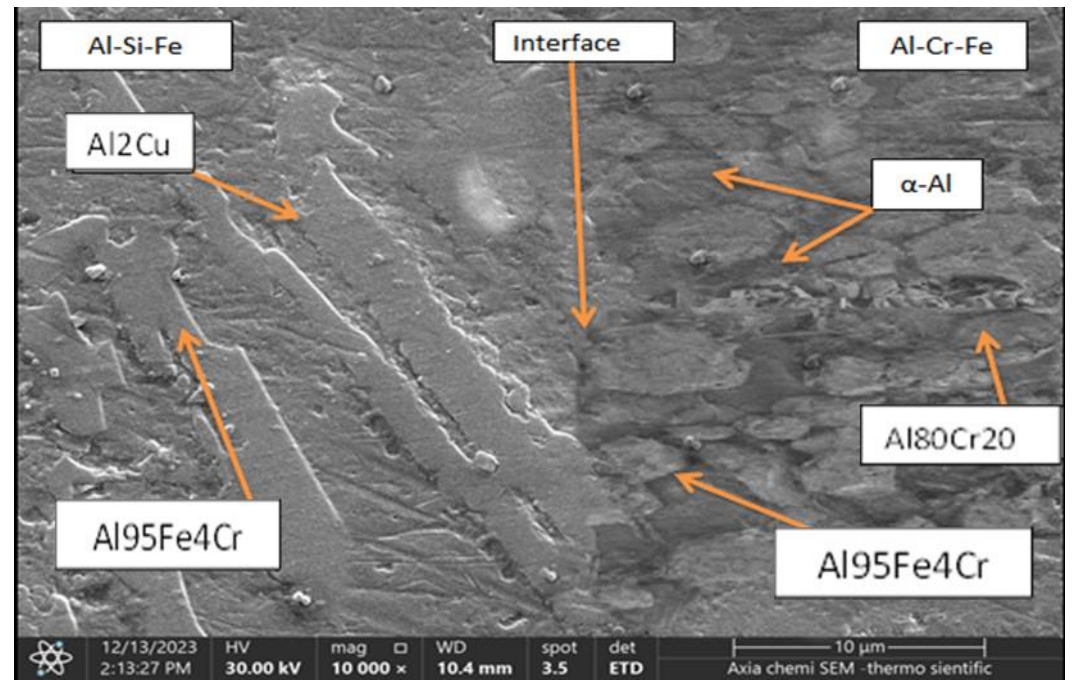


Figure 6. SEM image at interface of FG sample (C1-C3) without vibration

Figures (7) and (8) show the results of the ED S test at a distance of 5 micrometre on both sides of the interface. There is a difference in the concentration of elements before and after the interface. The reason is in the difference in the chemical composition of the alloy. The change in the distribution of elements in the alloy is almost

without vibration at a distance of 1 micrometre from each sides. From Interface, while when the vibration is affected, it is at a distance of approximately 2 micrometer from each side, where the concentration of elements overlaps in both alloys, which reduces the difference in properties. Thus, it is reflected in the performance of FGM.



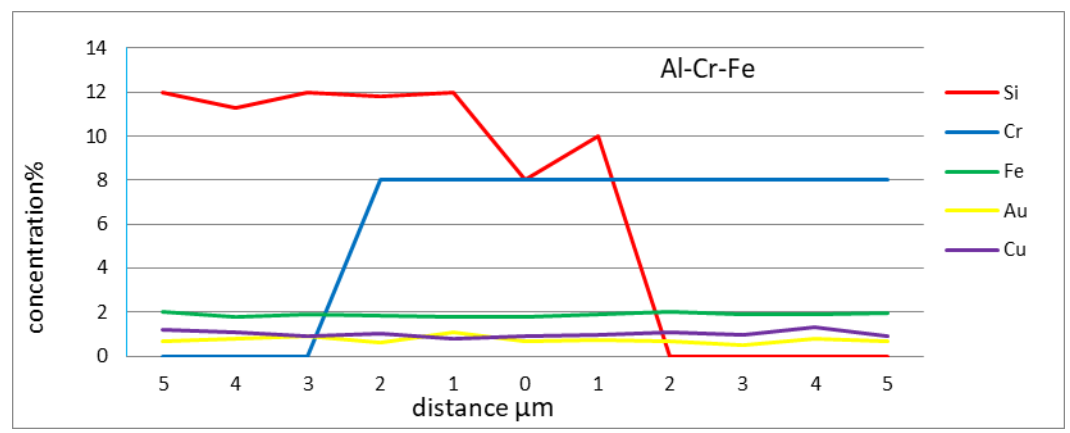


Figure 7. EDS FG sample (C1-C3) along interface at interface without vibration

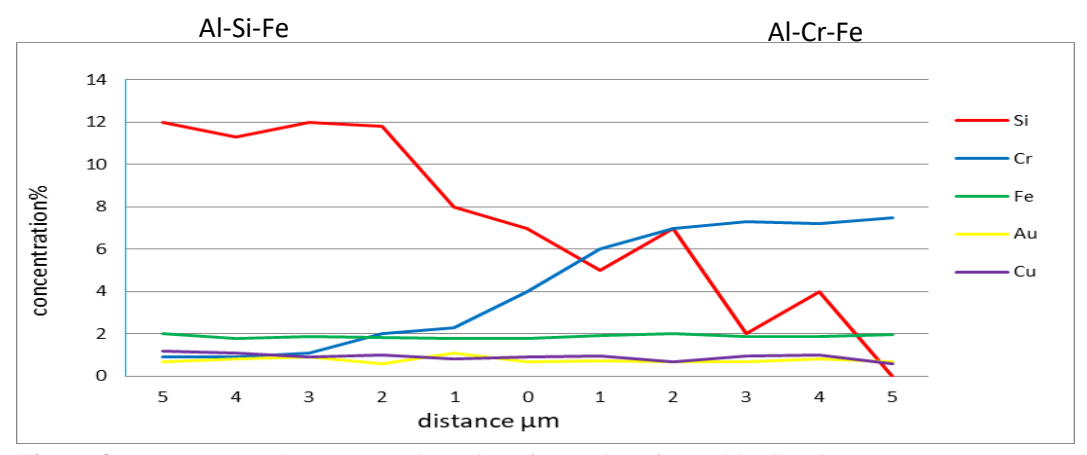


Figure 8. EDS FG sample (C1-C3) along interface at interface with vibration

4.4. Vickers Hardness Test

The results of Vickers hardness test for alloy samples are shown in Figure (9). Maximum hardness value in C1 alloy 178 HV and C3 98 HV without vibration, whale maximum hardness value in C1 alloy 174 HV and C3 96 HV with vibration. At interface there is a clear variation in hardness value between the two alloys at interface point, it caused by change in component and inter metallic for each alloy. Greatest value was recorded for C1 sample in A1-Si-Fe alloys, These increments could be attributed to the relatively high hardness of β -A15FeSi and Si in the alloy acting as barriers to dislocations motion.

Sample C3 in Al-Cr-Fe alloy present less value of hardness In comparison with Alloy C1 This could be attributed to the relatively high hardness of Cr component particles.

Figure (10) shows the Vickers hardness measurement for samples with and without the effect of vibration along the length of the test sample on both sides of the interface represented by the contact area of the two alloys that make up the

FGM. There is a clear difference in the hardness values, as the C1 alloy gave higher values than the C3 alloy, and this is expected as a result. The difference in chemical composition and thus the formation of compounds such as β-Al5FeSi and Al2Cu, which affect the hardness values, as they work to strengthen the spatial network by creating stresses within it or being obstacles to the movement of dislocations Al80Cr20, Al95Fe4Cr we note that The hardness of the samples under the effect of vibration is higher than that of samples without its effect, and this is due to the grans refinement and the reduction of pores and isolations as a result of the effect of vibration. On the other hand, the variation in hardness values along the surface of the alloy for the examined samples is small, as there is no significant difference between two successive points compared to samples without the effect of vibration. There is fluctuation in the values. The reason is that the effect of vibration leads to the distribution of elements evenly within the samples

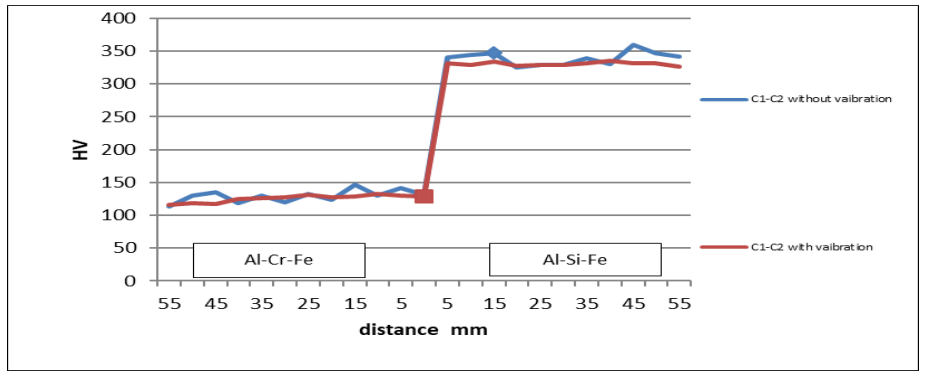


Figure 9. Vickers Hardness along FG samples

Figure (15) represents the Vickers hardness values on both sides of the interface. We notice a gradient in the hardness values from the C3 alloy

up to the C1 alloy. This is the result of the dissolution and mixing of the elements from the two alloys upon contact. The gradient in the hardness values for samples under the influence of vibration is smooth. The difference in hardness values along the examined points is small compared to samples without the effect of vibration, and as we mentioned previously, this is due to the homogeneous distribution of the elements and components of the alloy as a result of the effect of mechanical vibration.

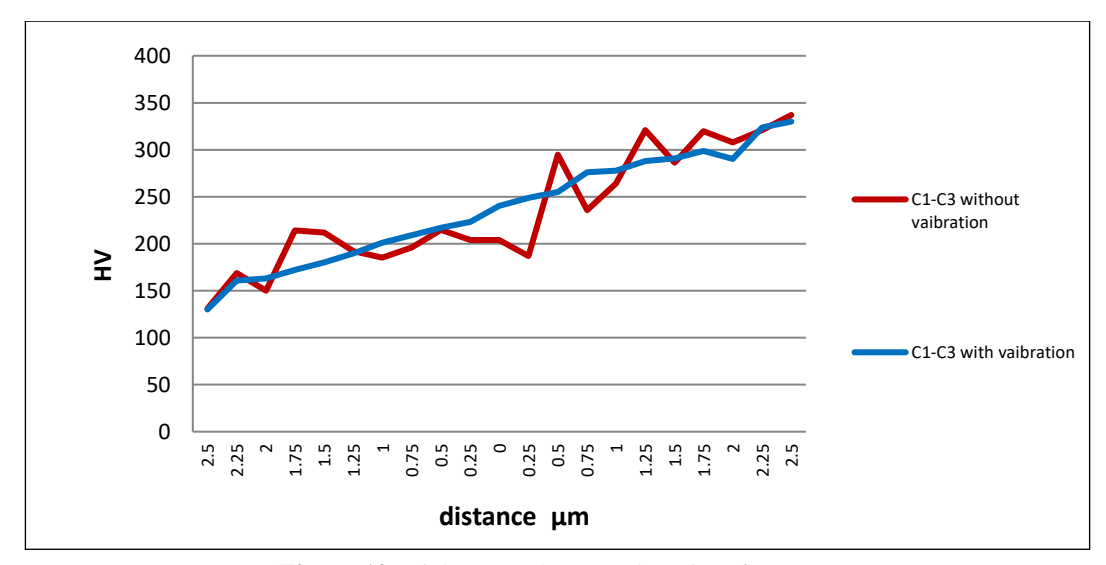


Figure 10. Vickers Hardness at along interface zone

5. Conclusions.

In this work, novel kinds of functionally graded materials realized by controlling the successional casting were produced. The alloy Al-Si-Fe was adopted along with the Al-Cr-Fe alloy, obtaining castings with good-quality and low retained defects. The Fe present was taken into account to increase the mechanical properties of the as-cast FGM, especially by nucleating the Al5feSi intermetallic phases in composition Al-Si-Fe alloy and Al95Fe4Cr in Al-Cr-Fe alloy. Functionally graded materials were castings produced were mechanically tested, and their microstructures were observed at the scanning electron microscope **SEM-EDS**

- Microstructures examine showed metallurgical bonded joints between the two alloys are solid with a continuous interface following consecutive gravity casting presented good bonding, which the mechanical testing's have highlighted.
- Moreover, SEM observations of the FGMs interfaces highlight, in general, the absence of extended defects. The two microstructures appear to be entirely different from one another in terms of

the microstructures of each of the two alloys far from the metallurgical junction.

- EDS shows variation of element along interface, the contrition change according addition to allovs.
- presence of iron-chromium aluminum alloy, which has intermetallic bonding well with the matrix."

Acknowledgments: The authors would like to reveal their appreciation and gratitude to the respected reviewers editors for and constructive comments.

References

- 1. Botero C., Koptyug A., Sjöström, W., Jiménez-Piqué E., Şelte A., & Rännar L. E. Functionally Graded Steels Obtained via Electron Beam Powder Bed Fusion. Key Engineering Materials 2023; 964: 79-84. https://doi.org/10.4028/p-xaC6qO
- Młynarek-Żak, K., Pakieła, W., Łukowiec, D., Bajorek, A., Gebara, P., Szakál, A. & Babilas, R. Structure and selected properties of Al-Cr-

ISSN: 2632-2714

Fe alloys with the presence of structurally complex alloy phases. Scientific Reports 2022; 12: 141-164. https://doi.org/10.1038/s41598-022-17870-0

- 3. Li, R., Yu, W., Zhang, Y., Li, C., Qu, Y., Nie, S., ... & Yu, B. Effect of phase proportion on wear behavior of Al–Cr–Fe–Ni dual-phase high entropy alloys. Metallography, Microstructure, and Analysis 2021; 10: 106-115. https://doi.org/ 10.1007/s13632-020-00709-3
- Yang, S., Lu, J., Xing, F., Zhang, L., & Zhong, Y. Revisit the VEC rule in high entropy alloys (HEAs) with high-throughput CALPHAD approach and its applications for material design-A case study with Al-Co-Cr-Fe-Ni system. Acta Materialia 2020; 192: 11-19.

https://doi.org/10.1016/j.actamat.2020.03.039

- Ribeiro, T. M., Catellan, E., Garcia, A., & dos Santos, C. A. The effects of Cr addition on microstructure, hardness and tensile properties of as-cast Al-3.8 wt.% Cu-(Cr) alloys. Journal of Materials Research and Technology2020;9(3), 6620-6631.https://doi.org/10.1016/j.jmrt.2020.04.054
- Koller, C. M., Kirnbauer, A., Hahn, R., Widrig, B., Kolozsvári, S., Ramm, J., & Mayrhofer, P. H. Oxidation behavior of intermetallic Al-Cr and Al-Cr-Fe macroparticles. Journal of Vacuum Science & Technology A 2017; 35(6).

https://doi.org/10.2139/ssrn.4705444

- 7. de Araujo, A. P., Micheloti, L., Kiminami, C. S., & Gargarella, P. Microstructure, phase formation and properties of rapid solidified Al–Fe–Cr–Ti alloys. Materials Science and Technology 2020;36(11), 1205-1214.https://doi.org/10.1080/02670836.2020. 1763555
- Švecová, I., Tillová, E., Kuchariková, L., & Knap, V. Possibilities of predicting undesirable iron intermetallic phases in secondary Al-alloys. Transportation Research Procedia 2021; 55, 797-804.https://doi.org/10.3390/electronicmat3010
- 9. Fracchia, E., Lombardo, S., & Rosso, M. Case study of a functionally graded aluminum part.

- Applied Sciences2018; 8(7), 1113https://doi.org/ 10.3390/app8071113
- Gao, T., Li, Z., Zhang, Y., Qin, J., & Liu, X. Phase evolution of β-Al 5 FeSi during recycling of Al–Si–Fe alloys by Mg melt. International Journal of Metalcasting 2019;13, 473-478 . https://doi.org/10.1007/s40962-018-0279-3
- 12. Wang, J., Liu, S., Bai, X., Zhou, X., & Han, X. Oxidation behavior of Fe–Al–Cr alloy at high temperature: Experiment and a first principle study. Vacuum, 173, 109144 (2020). https://doi.org/10.1016/j.vacuum.2019.109144
- Shi, H., Jianu, A., Fetzer, R., Szabo, D. V., Schlabach, S., Weisenburger, A., & Mueller, G. Compatibility and microstructure evolution of Al-Cr-Fe-Ni high entropy model alloys exposed to oxygen-containing molten lead. Corrosion Science 2021;189, 109593. https://doi.org/10.1016/j.corsci.2021.109593
- Que, Z., Wang, Y., Mendis, C. L., Fang, C., Xia, J., Zhou, X., & Fan, Z. Understanding Fe-containing intermetallic compounds in Al alloys: an overview of recent advances from the LiME research hub. Metals 2022;12(10), 1677. https://doi.org/10.3390/met12101677
- 15. Gao, T., Li, Z., Zhang, Y., Qin, J., & Liu, X. Phase evolution of β-Al 5 FeSi during recycling of Al–Si–Fe alloys by Mg melt. International Journal of Metalcasting 2019; 13, 473-478. https://doi.org/10.1007/s40962-018-0279-3
- Sheshukov, O. Y., & Kataev, V. V. Influence of Titanium and Zirconium on the Structure and Heat-Resistance of Low-Carbon Iron–Aluminum Alloys. Steel in Translation, 51, 621-626 (2021). https://doi.org/10.1179/174328407X168766
- Chen, H. Z., Li, B. R., Wen, B., Ye, Q., & Zhang, N. Q. Corrosion behaviours of iron-chromium-aluminium steel near the melting point of various eutectic salts. Solar Energy Materials and Solar Cells 2020; 210, 110510. https://doi.org/10.1016/j.solmat.2020.110510

ISSN: 2632-2714

- Behrens, B. A., Brunotte, K., Petersen, T., & Relge, R. Investigation on the Microstructure of ECAP-Processed Iron-Aluminium Alloys. Materials 2021;14(1), 219 . jhttps://doi.org/10.3390/ma14010219
- Siekaniec, D., Kopyciński, D., Tyrała, E., Guzik, E., & Szczęsny, A. Optimisation of solidification structure and properties of hypoeutectic chromium cast iron. Materials2022; 15(18), 6243 . https://doi.org/10.3390/ma15186243
- Babilas, R., Bajorek, A., Spilka, M., Radoń, A., & Łoński, W. Structure and corrosion resistance of Al–Cu–Fe alloys. Progress in Natural Science: Materials International 2020; 30(3), 393-401.https://doi.org/10.1016/j.pnsc.2020.06.00
- Pérez-Prado, M. T., Martin, A., Shi, D. F., Milenkovic, S., & Cepeda-Jiménez, C. M. An Al-5Fe-6Cr alloy with outstanding high temperature mechanical behavior by laser powder bed fusion. Additive Manufacturing 2022; 55, 102828.https://doi.org/10.1016/j.addma.2022.102828
- 22. Koller, C. M., Kirnbauer, A., Dalbauer, V., Kolozsvári, S., Ramm, J., & Mayrhofer, P. H. On the oxidation behavior of cathodic arc evaporated Al-Cr-Fe and Al-Cr-Fe-O coatings. I. Journal of Vacuum Science & Technology A2019; 37(4).https://doi.org/10.1116/1.5099123
- 23. Sourani, F., Enayati, M. H., & Ngan, A. H. W. On the in situ synthesis of (Fe, Cr) Al and (Fe, Cr) Al–Al2O3 nanostructured materials. Materials Research Express 2019;6(8), . https://doi.org/10.1088/2053-1591/ab24f5
- 24. Skorodzievskii, V. S., Ustinov, A. I., Polishchuk, S. S., Demchenkov, S. A., & Telychko, V. O. Dissipative properties of Al-(Fe, Cr) vacuum coatings with different composite structures. Surface and Coatings Technology 2019; 367, 179-186. https://doi.org/ 10.1016/j.surfcoat.2019.03.074
- Rehman, A., Shah, S. A. H., Nizamani, A. U., Ahsan, M., Baig, A. M., & Sadaqat, A. (2024). AI-Driven Predictive Maintenance for Energy Storage Systems: Enhancing Reliability and Lifespan. PowerTech Journal,

- 48(3). https://doi.org/10.XXXX/powertech.v48.113 ​:contentReference[oaicite:0]{index= 0}
- Muneer, B. A. I. G., Ammar, H. R., Seikh, A. H., Mohammed, J. A., Fahad, A. M., & Alaboodi, A. Thermal stability of nanocrystalline Al– 10Fe– 5Cr bulk alloy. Transactions of Nonferrous Metals Society of China 2019; 29(2), 242-252. https://doi.org/10.1016/S1003-6326(16)64128-6
- Shockner, R., Edry, I., Pinkas, M., & Meshi, L. Systematic study of the effect of Cr on the microstructure, phase content and hardness of the AlCrxFeCoNi alloys. Journal of Alloys and Compounds 2023; 940, 168897.https://doi.org/10.1116/1.5099123